Uncertainty Visualization of Ensemble Hemodynamic Simulations for a Cerebral Bifurcation Aneurysm

Saalfeld S.[1], Berg P.[2], Hirsch J.[1], Preim B.[1]

[1]OvG-University, Department of Simulation and Graphics, Magdeburg, Germany
[2]OvG-University, Department of Fluid Dynamics and Technical Flows, Magdeburg, Germany

Kontakt: sylvia.saalfeld@ovgu.de

Abstract

Computational Fluid Dynamics allows for blood flow simulations of intracranial aneurysms to support the decision making process of a clinical expert. Due to missing information, e.g. the lack of patient-specific boundary conditions, simulations depend on certain approximations, which induce uncertainty into the results. We focus on the influence of varying outflow boundary conditions for a realistic bifurcation aneurysm of the middle cerebral artery. To obtain uncertainty information, an ensemble simulation is carried out where the outflow boundary conditions were systematically altered to account for possible flow scenarios. For an analysis of the simulation results, we develop uncertainty visualizations to identify the aneurysm parts that strongly depend on the boundary conditions.

Keywords: uncertainty visualization, CFD, cerebral aneurysm

1 Problem

For the rupture risk of cerebral aneurysms, morphological parameters as well as the internal blood flow is evaluated. Computational Fluid Dynamics (CFD) allows for the simulation of the individual blood flow. However, due to missing information, e.g., patient-specific inflow and outflow waveforms, parameters and boundary conditions are often approximated using steady flow conditions or applying literature values to the simulation domain. As a consequence, such assumptions induce uncertainty into the simulation results.

We focus on the influence of boundary conditions regarding a patient-specific bifurcation aneurysm located at the middle cerebral artery (MCA). We carry out an ensemble simulation comprising a patient-specific inflow boundary condition, but varying outflow conditions to account for different flow-splitting scenarios.

For the inspection of the resulting simulations, we develop 3D uncertainty visualizations, which depict portions of the aneurysm with large variations due to the different input parameters. Uncertainty visualizations are often used for weather or climate modeling, where the view of simulation results is altered to account for the assigned uncertainty [1][2]. The uncertainty can be approximated with probability distributions based on repeated measurements or simulations. The visualization of such uncertain values, i.e., values with increased variance, often comprises transparency, reduced saturation or animation [3].

In contrast, we focus on strong variations due to the adapted outflow conditions. Especially irregular and complex blood flow is associated with increased aneurysm rupture risk [4]. Thus, regions characterized by strong variations, which are sensitive to input parameters, are from utmost interest. Our 3D visualizations highlight these regions and omit parts that remain the same for all simulation results and do not depend on the varied input parameters.

2 Material and Methods

This section describes the underlying patient data and the hemodynamic simulations. Afterwards, the uncertainty visualization techniques are explained.

2.1 Case Description and Data Extraction

A 77-year-old female patient underwent a medical check-up of the brain, and magnetic resonance (MR) angiography revealed an unruptured aneurysm (approximately 10 mm in diameter) at the bifurcation of the left MCA. Thereafter, the patient was followed up by MR angiography at 6-month intervals. Gradual growth of the aneurysm was observed during a 5-year follow-up. Its form changed from spherical to irregular shape. Coil embolization was performed, considering the risk of rupture. Image acquisition was performed by using 3D digital subtraction angiography. The aneurysm segmentation was carried out using MeVisLab 2.8 (MeVis Medical Solutions AG, Bremen, Germany) with a threshold-based segmentation approach [5]. A neuroradiologist reviewed the virtual geometry afterwards to check the plausibility of the reconstructed shape. The investigated case including the inlet (red) and outlet (blue) cross-sections is shown in Figure 1.

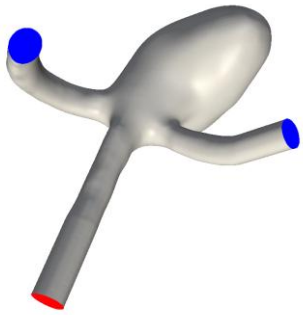

Figure 1: Depiction of the cerebral aneurysm model with color-coded inlet (red) and outlets (blue).

2.2 Hemodynamic Simulation

In order to carry out realistic blood flow simulations, spatial discretization of the aneurysm surface model was required. In this regard, CD-Adapco StarCCM+ 10.04 (Siemens Product Lifecycle Management Software Inc., Plano, TX, USA 75024) was used to generate polyhedral elements (base size = 0.1 mm). To appropriately resolve the steep velocity gradients occurring near the vessel wall, four prism layers with a base size of 33 μm were inserted. The final mesh consisted of 0.8 million elements.

Patient-specific inflow boundary conditions were measured during the intervention using 2D phase contrast magnetic resonance imaging (PC-MRI) on a 3T whole-body MRI scanner (Signa HDxt; GE Healthcare Japan, Tokyo, Japan). The measurement was ECG-triggered and the standard 2D cine PC-MRI sequence was carried out with 0.3 mm in-plane resolution and 30 phases in order to have sufficient resolution for the time-dependent velocities. The period of the cardiac cycle was 0.925 s with a cycle-averaged cross section-mean velocity (and Reynolds number) of 0.47 m/s (Re = 267). This value was applied to the inlet to perform steady-state computations.
To account for possible flow differences, outlet boundary conditions were varied according to the following protocol: A) zero-pressure conditions for both outlets, B-H) equivalent flow-splitting between the outlets applying the ratios 20%-80% to 80%-20% with a 10 percentage stepping, see Figure 2. The variations yield different simulation results and subsequently different flow parameter values. In Figure 2, the parameter wall shear stress (WSS) is color-coded with a rainbow color map on the aneurysm surface.

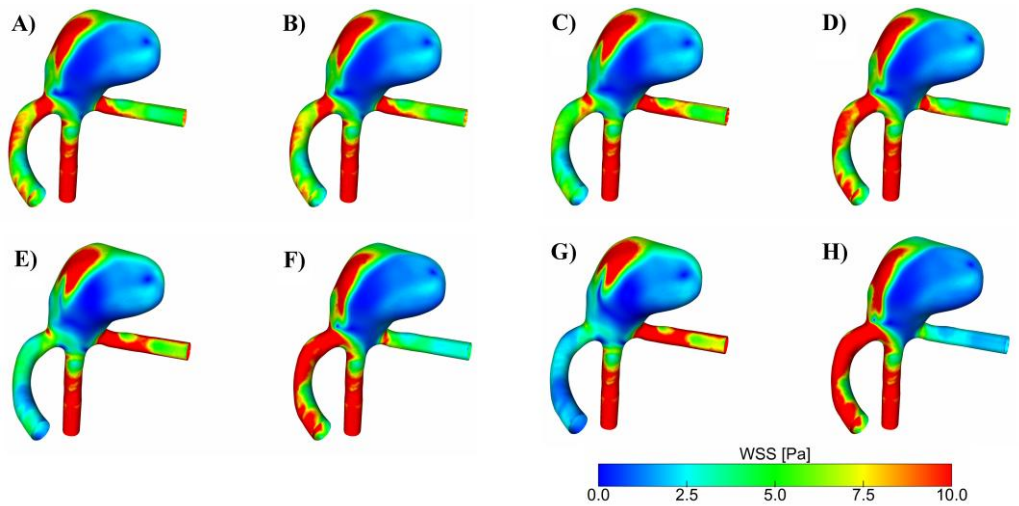

Figure 2: Illustration of the eight blood flow scenarios: A) zero-pressure outlets, B) outflow-splitting: 50%-50%, C) outflow-splitting: 40%-60%, D) outflow-splitting: 60%-40%, E) outflow-splitting: 30%-70%, F) outflow-splitting: 70%-30%, G) outflow-splitting: 20%-80%, H) outflow-splitting: 80%-20%. The wall shear stress (WSS) is color-coded with a rainbow color map.

In all eight simulations, StarCCM+ 10.04 was used, while blood was assumed to be an incompressible (ρ=1055 kg/m^3), laminar, Newtonian (η=4 mPa·s) fluid. Convergence was obtained when the scaled residuals for continuity and all velocity components decreased below a value of 1e-5.

2.3 Uncertainty Visualization

We present uncertainty visualizations to highlight variations based on the eight simulation results. Our prototype is implemented in C++ and uses the Visualization Toolkit 6.3.0 (VTK, Kitware Inc., Clifton Park, NY, USA, http://vtk.org). For each vertex, the mean and standard deviation of the scalar parameters pressure and velocity magnitude are extracted. If there are strong variations, i.e., an increased standard deviation, the information for this vertex is considered as very uncertain. In contrast, very small standard deviation values indicate similar simulation results for the varying outlets and thus very small uncertainty. We provide our results via 3D direct volume rendering (DVR). Thus, the user can easily detect portions of the data with strong variations in 3D.

For the approximation of the velocity direction's uncertainty, we extract the mean vector from the eight direction vectors. Next, we extract the largest possible angle between the mean vector and the eight direction vectors. Large angles indicate increased uncertainty, i.e., strong variations of the flow directions. Small values indicate similar results for the directions and thus a low uncertainty.

Based on the extracted uncertainty information, we provide 3D uncertainty visualizations for the clinical expert; see the example for the velocity's magnitude in Figure 3. To highlight areas with strong variations, we employ the velocity's standard deviation for the opacity transfer function, see Figure 4. Thus, vertices with increased uncertainty are mapped more opaquely. The amount of the average velocity's magnitude is color-coded based on the color map presented in Figure 4. The divergent color map was tailored for scientific visualization by Moreland et al. [6].

Figure 3: 3D uncertainty visualization of the velocity magnitude. There is a strong variation considering the aneurysm's inflow zone (arrow) as well as inside the aneurysm head (arrowhead).

In accordance to the representation of the uncertainty regarding the scalar parameter velocity magnitude, uncertainty visualization for the scalar parameter pressure is obtained, see Figure 5. The same color map is employed for pressure and velocity magnitude and increasing values for pressure's standard deviation lead to increased opacity (recall Fig. 4). For the visualization of the velocity direction, our color-coding was inspired by the illustration of fiber tracts based on diffusion tensor MR imaging [7]. Hence, the average direction approximated from the eight simulation results is color-coded with a directional color map, see Figure 6. Again, the opacity transfer function assigns full transparency to portions of the data where the standard deviation equals zero and assigns increasing opacity to increasing standard deviation values.

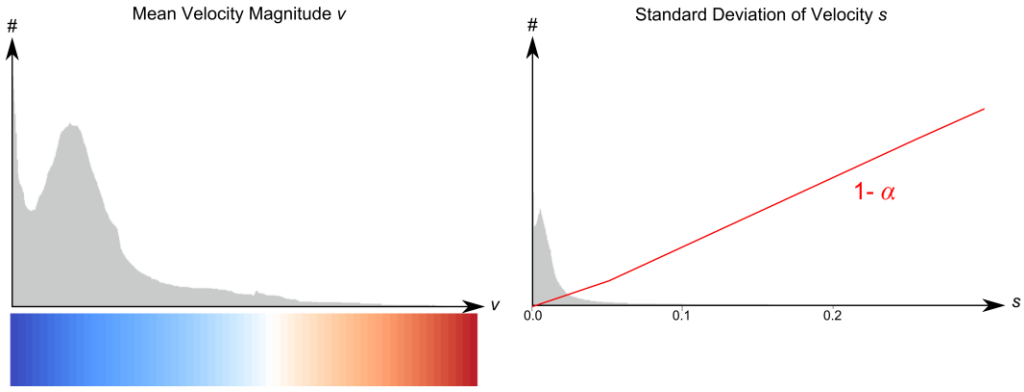

Figure 4: The color scale maps the average velocity magnitude to color (left). The opacity transfer function (right) assigns transparency (α) to vertices with zero standard deviation and increased opacity to increased standard deviation values.

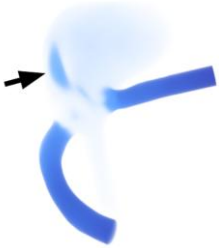

Figure 5: Depiction of the pressure variation. Beyond the outlets, a region at the aneurysm surface is present (arrow).

With these design choices, the attention of the expert is guided towards the more certain (reliable) information whereas the attenuated highly uncertain information is perceived as a context. In contrast to many uncertainty visualizations, we do not introduce additional graphical primitives that often lead to visual clutter.

The developed uncertainty visualization allows for the identification of regions with strongest variations and thus strongest dependency on the varied input parameters.

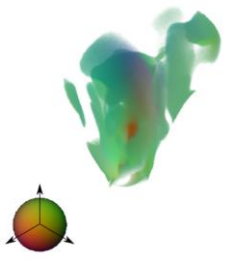

Figure 6: Depiction of the average velocity direction. Variations of velocity are irregular and complex.

3 Results

When analyzing the velocity magnitude variations, two regions become visible, recall 0Especially the aneurysm's inflow zone is characterized by strong varying and large velocity magnitude values, i.e., opaque and red-colored regions. Furthermore, a second region becomes visible inside the aneurysm head.

When comparing the pressure variations, no strong dependency is present regarding the aneurysms inflow zone. However, a region on the aneurysm surface is present, recall **Fehler! Verweisquelle konnte nicht gefunden werden.**We further examine this region by combining pressure, velocity magnitude and color-coded WSS surface presentations, see **Fehler! Verweisquelle konnte nicht gefunden werden.**Interestingly, the region on the aneurysm with increased WSS is also characterized by increased pressure and velocity variations. Thus, this result may be error-prone. Evaluation of the velocity directional variation yields three suspect regions, see Figure 8. These regions are also characterized by velocity magnitude variations but rather moderate pressure variations. The transfer function was adapted to provide information for all three regions.

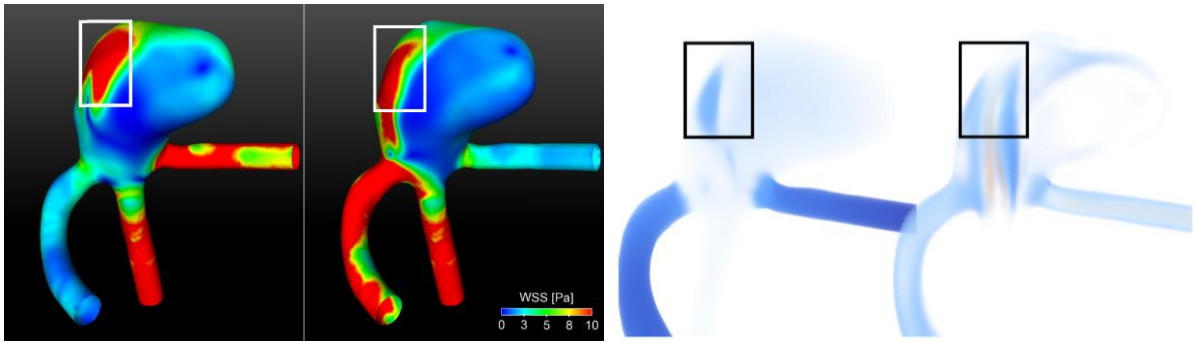

Figure 7: Color-coded 3D surface visualization to depict the WSS for configuration H (i.e. 80% vs. 20%) and configuration G (i.e. 20% vs. 80%) at the left. At the middle-right, the 3D DVR view of the pressure variation is shown and the velocity magnitude variation is displayed on the right. The region with largest WSS (marked with the rectangle) is characterized by uncertain pressure and velocity values.

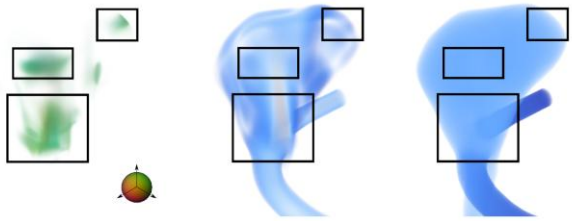

Figure 8: Visualization of the velocity direction reveals three regions with strong variations (left). These regions are also characterized by strong velocity magnitude variations (center) but only moderate pressure changes (right). The transfer function of the pressure view was adapted such that for each region the average pressure value is shown.

4 Discussion

With the presented uncertainty visualization techniques depending on mean and standard deviation, it is possible to reveal regions of the aneurysm with strongest variations of parameter values. Hence, we are focusing on the spatial identification of regions that strongly depend on the approximated input parameters. In contrast, the evaluation of internal blood flow can be carried out based on streamlines and streamline clusters. Ferstl et al. [8] developed streamline variability plots to characterize uncertainty in vector field ensembles. They also provide an uncertainty visualization for time-dependent vector fields [9], an approach which may be adapted to time-dependent simulation results of internal aneurysm blood flow in future. Our previous work [10] includes 2D uncertainty visualizations of time-dependent WSS values. For future work, the ensemble simulation could

comprise unsteady simulations yielding time-dependent WSS values, which could be combined with the presented 3D DVR views for further evaluation of parameter dependency.

5 Conclusion

In conclusion, we strongly recommend substituting single CFD results for internal blood flow prediction in cerebral aneurysms with ensemble simulations. The systematic variation of approximated input parameters provides valuable information about input-sensitive aneurysm parts of the simulated blood flow. With the presented 3D uncertainty visualizations, these parts can be identified.

The combination of the different visualizations allows for combined inspection, e.g., for regions with large variations of pressure, the underlying velocity magnitude and direction variation can be examined.

Acknowledgment

This work was partially funded by the Federal Ministry of Education and Research within the Forschungscampus *STIMULATE* (grant number '13GW0095A').

References

[1] K. Pöthkow, H.-C. Hege, "Positional Uncertainty of Isocontours: Condition Analysis and Probabilistic Measures", *IEEE Transactions on Visualization and Computer Graphics (TVCG)*, vol. 17, no. 10, pp. 1393–1406.

[2] K. Potter, A. T. Wilson, P.-T. Bremer, D. N. Williams, C. M. Doutriaux, V. Pascucci, and C. R. Johnson, "Ensemble-Vis: A Framework for the Statistical Visualization of Ensemble Data", *Proc. of ICDM Workshops*, pp. 233-240, 2009.

[3] K. Brodlie, and A. R. Osorio, and A. Lopes, "A Review of Uncertainty in Data Visualization", in John Dill, Rae Earnshaw, David Kasik, John Vince and Pak Chung Wong (Eds.): Expanding the Frontiers of Visual Analytics and Visualization, Springer Verlag London, pp. 81–109, 2012.

[4] J. R. Cebral, M. A. Castro, S. Appanaboyina, C. M. Putman, D. Millan, and A. F. Frangi, "Efficient Pipeline for Image-Based Patient-Specific Analysis of Cerebral Aneurysm Hemodynamics: Technique and Sensitivity", *IEEE Transactions on Medical Imaging*, vol. 24 no. 4, pp. 457–467, 2005.

[5] S. Glaßer, M. Neugebauer, P. Berg, B. Preim, "Reconstruction of 3D Surface Meshes for Bood Flow Simulations of Intracranial Aneurysms", in Proc. of Jahrestagung der Deutschen Gesellschaft für Computer- und Roboterassistierte Chirurgie (CURCA), pp. 163-168, 2015.

[6] K. Moreland, "Diverging Color Maps for Scientific Visualization, in Proc. of the 5th International Symposium on Advances in Visual Computing: Part II. Berlin, Heidelberg : Springer-Verlag, pp. 92-103, 2009.

[7] W. Benger, H. Bartsch, H.-C. Hege, H. Kitzler, A. Shumilina, A. Werner, "Visualizing Neuronal Structures in the Human Brain via Diffusion Tensor MRI", *International Journal of Neuroscience*, vol. 116, no. 4, pp. 461–514, 2006.

[8] F. Ferstl, K. Bürger, and R. Westermann, "Streamline Variability Plots for Characterizing the Uncertainty in Vector Field Ensembles", *IEEE Transactions on Visualization and Computer Graphics (TVCG)*, vol. 22, no. 1, pp. 767-776, 2016.

[9] F. Ferstl, M. Kanzler, M. Rautenhaus, and R. Westermann, "Time-Hierarchical Clustering and Visualization of Weather Forecast Ensembles", *IEEE Transactions on Visualization and Computer Graphics (TVCG)*, vol. 23, no. 1, pp. 831-840, 2017.

[10] S. Glaßer, J. Hirsch, P. Berg, P. Saalfeld, O. Beuing, G. Janiga, and B. Preim, "Evaluation of Time-Dependent Wall Shear Stress Visualizations for Cerebral Aneurysms", in *Proc. of Bildverarbeitung für die Medizin (BVM)*, pp. 236-241, 2016.